

Acoustic characterization of sound absorbing natural fibres

Pedrosa, A. M.¹, Sánchez-Orgaz, E. M.², Denia, F. D.³, Fuenmayor, F. J.⁴
Centro de Investigación en Ingeniería Mecánica, Universitat Politècnica de València
Camino de Vera s/n, 46022 Valencia, Spain

ABSTRACT

Some synthetic materials commonly used in noise control systems, such as absorbent fibres, can have a potential harmful effect on human health and the environment. For this reason, searching of new sound absorbent materials is an active field of research. In the current work, natural fibres are presented as a potential alternative to the traditional fibrous materials, since the sound attenuation performance of the former can be good and these fibres can also be easily recycled from industrial scrap. The main goal of this work is the acoustic characterization of natural fibres. The procedure here proposed focuses on measuring the flow resistivity of these materials through a steady flow experimental setup. This technique has been previously implemented by the authors, showing good agreement with theoretical models for fibreglass. Finally, a Delany and Bazley type theoretical acoustic model is proposed for coconut and sisal fibres through an experimental curve fitting method, since the results available in the bibliography are not accurate enough. Also, these properties are validated by comparing experimental measurements of the transmission loss (*TL*) of a silencer prototype with FEM computations.

Keywords: Natural fibres, Flow resistivity, Measurement, Acoustic properties
I-INCE Classification of Subject Number: 35

1. INTRODUCTION

According to the World Health Organization, nowadays noise is one of the most widespread forms of environmental pollution, as it has harmful effects on health [1]. For this reason, the use of noise control devices is essential, as it is the case of silencers [2] [3].

¹ anpedsan@dimm.upv.es

² evsncor@upvnet.upv.es

³ fdenia@mcm.upv.es

⁴ ffuenmay@mcm.upv.es

The air conditioning systems on buildings consist of fans, ducts, area changes, as well as gates and other elements needed for the air renewal generating noise during the process. For this reason, it is necessary to provide them with noise control elements and devices such as silencers, which reduce the level of sound produced [3] - [5]. Traditionally, dissipative silencers usually contain synthetic materials, such as fibreglass or rockwool [2], [3]. However, this type of fibres can be pollutant due to the drag produced by the air flow [6] - [9]. For this reason, the use of natural fibres with relatively large diameter in this kind of systems can be interesting.

The natural fibres considered in this work have the advantage of being less polluting to the environment since they are biodegradable.. Additionally, fibres from industrial scrap that would otherwise be wasted, could be used. Another additional advantage is the potential increase in income of producing countries [10], [11].

2. ACOUSTICAL MODEL

In recent works [12] the two-source method with simultaneous excitation [13] has been successfully used to obtain the wavenumber \tilde{k} and the characteristic acoustic impedance \tilde{Z} of both synthetic and natural fibres. The former was Owens Corning's texturized Advantex fibreglass and the latter coconut and a mixture of coconut-sisal fibre. The experimental results were compared with the well-known Delany and Bazley model [14],

$$\tilde{k} = k_0 \left(1 + a_3 \left(\frac{f \rho_0}{R_f} \right)^{-a_4} - j a_1 \left(\frac{f \rho_0}{R_f} \right)^{-a_2} \right) \quad (1)$$

$$\tilde{Z} = Z_0 \left(1 + a_5 \left(\frac{f \rho_0}{R_f} \right)^{-a_6} - j a_7 \left(\frac{f \rho_0}{R_f} \right)^{-a_8} \right) \quad (2)$$

where $k_0 = \omega/c_0$ is the air wavenumber, $Z_0 = \rho_0 c_0$ is the air characteristic impedance, $\omega = 2\pi f$ is the angular frequency, f is the frequency, c_0 is the speed of sound, ρ_0 is the air density and R_f the static flow resistivity of the absorbent material.

The coefficients a_i and the static flow resistivity of the synthetic fibre employed are published in previous works [15]. Thus, the experimental results obtained in [12] could be compared with theoretical predictions showing good agreement.

However the same parameters for natural fibres are less known. Garai [16] obtained experimentally the optimal value of coefficients a_i of Equations 1 and 2 for different polyester fibres. Later, Berardi [17] measured the sound absorption coefficient and the static flow resistivity of natural fibres and compared the experimental results with theoretical models employing the Garai's coefficients because the mean diameter and the density of polyester are close enough to the tested fibres. The conclusion of [17] was that theoretical models allow to predict the general trend, but they could not be accurate enough due mainly to the high heterogeneity of the physical properties of natural fibres. For this reason, in the previous work of the authors [12], only the measurements of coconut fibre was compared with the theoretical predictions with the coefficients provided by Garai.

Regarding the static flow resistivity of coconut fibre, the value $R_f = 1500 \text{ N s/m}^4$ measured by Berardi [17] was employed in [12], corresponding to the mean value of fibre density $\rho_f = 60 \text{ kg/m}^3$. In the case of a different density of coconut fibre and coconut-sisal fibre, the measurements showed similar behaviour and an expected trend since the attenuation increases with the density of fibre. Finally a prototype of a dissipative silencer with coconut fibre with $\rho_f = 60 \text{ kg/m}^3$ was constructed and its TL was measured. The experimental TL was compared with the numerical calculations with

the Garai coefficients showing fairly close values. Additionally, the results supported that the coconut and coconut-sisal fibres present acoustic properties that make them potential candidates for uses in acoustic attenuation devices.

Therefore the scope of this work is to obtain a proper model of the acoustic behaviour for coconut and coconut-sisal fibres, first measuring experimentally the static flow resistivity and later computing the Delany and Bazley coefficients by a semi-empirical curve fitting method. The latter has been carried out through an optimization procedure using a genetic algorithm, since this has been proved to be efficient and robust when finding the optimal solution [8].

3. EXPERIMENTAL SET-UP

3.1 Static flow resistivity

The static airflow resistivity is defined as the ratio between the pressure drop ΔP and the flow velocity v through a layer of material multiplied by the thickness of the specimen d .

$$R_f = \frac{\Delta P}{d \cdot v} \quad (3)$$

It is commonly expressed in $N s/m^4$. Equations 1 and 2 show that the acoustic response of fibrous materials is highly dependent on their airflow resistance values. Increasing values of resistivity generally imply a higher absorption of acoustic energy, until a saturation phenomenon occurs due to the reduction of interstices of the fibre.

In this work the air flow resistivity is measured by a direct method based on the standardized procedure [18].

The experimental set-up to measure the static flow resistivity (Figure 1a)) is based on the standardized direct method [18]. The equipment consists of a blower that produces air flow at different velocities, a Pitot tube for measuring the air flow velocity and a differential manometer that measures the pressure drop across the specimen. Figure 1b) shows a specimen of coconut fibre. To avoid dragging the fibres, a tubular grid have been used.

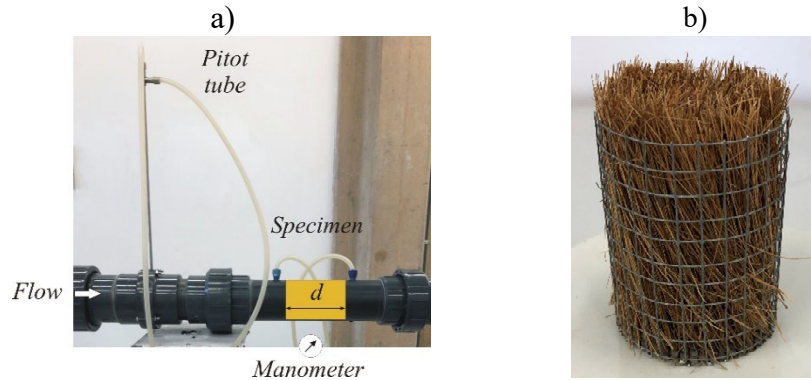


Figure 1 a) Experimental set-up for determining static flow resistivity by direct method, b) specimen.

Due to the physical limitations of the equipment employed for producing air flow at $v = 0.5$ mm/s, according to [18] a stepwise down airflow has been used. The static flow resistivity has been determined by extrapolating to $v = 0.5$ mm/s. Figure 2 shows the results for coconut fibre ($\rho_f = 87$ kg/m³) giving $R_f = 1695$ N s/m⁴ for this particular material sample.

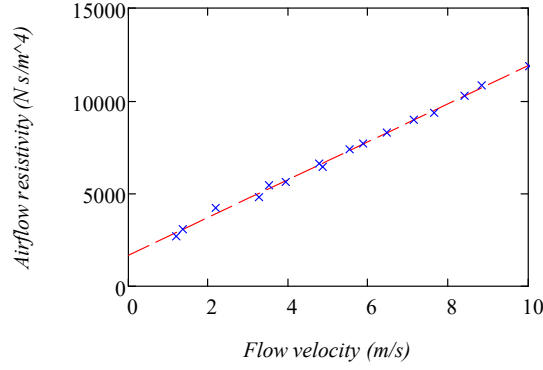


Figure 2 Static airflow resistivity of coconut fibre with $\rho_f = 87 \text{ kg/m}^3$;
 x x, measurements; - - -, linear regression.

Table 1 shows the static airflow resistivity obtained from measurements for two different natural fibres and density. For each result, two tests have been done, giving similar results. The results on Table 1 correspond to the mean value of the two tests at 25°C.

Table 1 Static airflow resistivity for natural fibres.

	Density (kg/m ³)	Static airflow resistivity (N s/m ⁴)
Coconut fibre	41.36	402.65
	87.29	1707.97
Coconut-sisal fibre	55.23	620.57
	95.15	1749.8

The experimental results obtained in this work are consistent with those obtained by Berardi and Iannace [17] and Del Rey et al. [19].

For different density or temperature, the resistivity can be estimated with the following equations [6] [20]

$$R_{T_0} = A_1 \rho_f^{A_2} \quad (3)$$

$$R_T = \left(\frac{T}{T_0}\right)^{0.6} R_{T_0} \quad (4)$$

where the coefficients A_1 and A_2 of Equation 3 are fitted from the experimental values on Table 1, R_{T/T_0} is the resistivity at absolute temperatures T/T_0 respectively. Table 2 shows the values for natural fibres at $T_0 = 298.15 \text{ K}$.

Table 2 Coefficients of static airflow resistivity of natural fibres.

	A_1	A_2
Coconut fibre	0.30006	1.93473
Coconut-sisal fibre	0.29809	1.90525

3.2 Two source method with simultaneous excitation

An in-duct acoustic system can be modelled with its transfer matrix [21] that relates two state variables in both sides of the element under study. For a uniform rigid duct (Figure 3) the transfer matrix referred to pressure p and particle velocity v , corresponds to the following expression

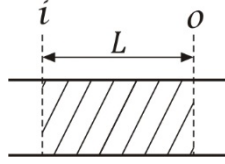


Figure 3 Uniform rigid duct.

$$\begin{Bmatrix} p \\ v \end{Bmatrix}_i = \begin{bmatrix} \cos(kL) & j Z \sin(kL) \\ \frac{j \sin(kL)}{Z} & \cos(kL) \end{bmatrix} \begin{Bmatrix} p \\ v \end{Bmatrix}_o \quad (5)$$

where $k = 2\pi f/c$ is the wavenumber, f is the frequency, c is the speed of sound, L is the length of the duct, j is the imaginary unit, $Z = \rho c$ is the characteristic impedance and ρ is the density of the medium (same for k , c and Z).

In this work, the transfer matrix of a duct filled with the absorbent material has been obtained by means of the two source method with simultaneous excitation. Further information of the methodology can be found in [12]. Figure 4 shows the sketch of the set-up.

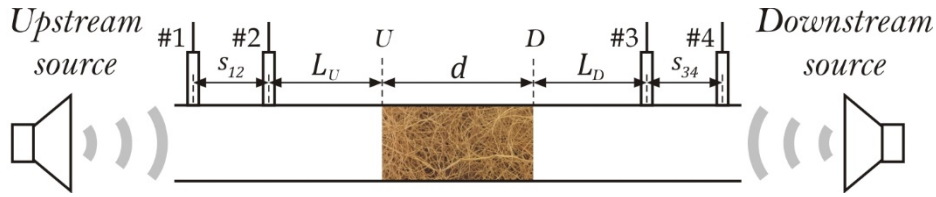


Figure 4 Two source method with simultaneous excitation.

The obtained transfer matrix relates pressure and velocity between sections U and D on Figure 4. Thus, taking into account Equation 5, the equivalent impedance \tilde{Z} and wavenumber \tilde{k} of the specimen can be calculated as follows

$$T_{1,1_m} = \cos(\tilde{k}d) \rightarrow \tilde{k} = \frac{\arccos(T_{1,1_m})}{d} \quad (6)$$

$$\frac{T_{1,2_m}}{T_{2,1_m}} = \tilde{Z}^2 \rightarrow \tilde{Z} = \sqrt{\frac{T_{1,2_m}}{T_{2,1_m}}} \quad (7)$$

where T_{i,j_m} is the term i, j of the transfer matrix defined in Equation 5.

4. ACOUSTIC CHARACTERIZATION

4.1 Material model

An absorbent material can be modelled through its equivalent acoustic properties, such as the characteristic impedance \tilde{Z} and wavenumber \tilde{k} . These properties can be modelled by the empirical expressions of Delany and Bazley described in Section 1 and here repeated for the sake of clarity

$$\tilde{k} = k_0 \left(1 + a_3 \left(\frac{f \rho_0}{R_f} \right)^{-a_4} - j a_1 \left(\frac{f \rho_0}{R_f} \right)^{-a_2} \right) \quad (1)$$

$$\tilde{Z} = Z_0 \left(1 + a_5 \left(\frac{f \rho_0}{R_f} \right)^{-a_6} - j a_7 \left(\frac{f \rho_0}{R_f} \right)^{-a_8} \right) \quad (2)$$

The coefficients and exponents of the previous equations a_i can be obtained by fitting a curve to the experimental data, since they depend on the fibre considered. In these case, they are fitted by means of an optimization process detailed in Section 3.2.

4.2 Optimization of Delany&Bazley's coefficients

The coefficients corresponding to the Delany and Bazley's model are here obtained for the different fibres under study through an optimization procedure, whose scheme is presented in Figure 5. The coefficients are the input variables of the process. In the present work, they are allowed to vary between a lower and an upper bound of 0.01 and 1, respectively, while the incremental step is 0.0001.

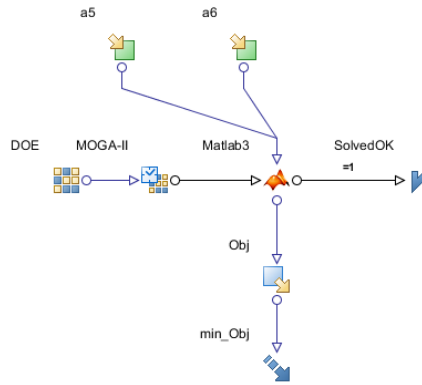


Figure 5 Scheme of the optimization process.

The optimization has been carried out by means of a genetic algorithm, whose main advantage is that it can escape from local optima and make a wide search within the design space. Besides it is not affected by pollution generated during the process. This method works with a population of solutions, called individuals, which make an effort to survive and reproduce. The basic unity of evolution is the individual, who is characterized by its genome. Computation time is divided into discrete steps, called generations. In each generation new individuals are generated (offspring) by recombination and mutation from their parents (the individuals of the previous generation). Each individual is evaluated in the environment by means of the assignment of a strength or health measurement (fitness). The main goal of the algorithm is finding the maximum strength.

In the current work, the algorithm used is MOGA-II (Multi-Objective Genetic Algorithm), which belongs to the commercial program modeFRONTIER[®]. It is a genetic algorithm for multiple objectives, nevertheless considering several objectives reduces the computation speed. For this reason, in the current study, only one objective has been used. The function under study is the difference between the characteristic impedance and wavenumber experimentally obtained with those results computed by their respective Delany and Bazley's models. However, these results depend on the frequency and for this reason, the average value has been obtained to evaluate the results in the whole frequency range of interest. Thus, this is the function to minimize, since the difference has to be as low as possible. It should be also noticed that minimizing the average value can be not the best choice because there can be a considerable dispersion of the results. Therefore, the standard deviation of the results is also processed and added to the previous average value in order to avoid undesirable solutions considering a single objective function to speed up the computations [8].

5. RESULTS

5.1 Experimental results

In this section the experimental results are presented. Four optimization analyses have been carried out for each fibre. The first two computations carried out allowed

to obtain the coefficients for the real and the imaginary part of the characteristic impedance in an independent way, while the other two allowed to calculate those belonging to the wavenumber.

For validating the procedure the measurements of fibreglass are compared with the Delany&Bazley model with the coefficients obtained by means of optimization. The same model but with the coefficients employed in previous works is also compared.

5.1.1 Validation

The coefficients shown on Table 3 correspond to Delany&Bazley's model.

Table 3 Comparison of Delany&Bazley's coefficients for Owens-Corning fibreglass.

	a_1	a_2	a_3	a_4	a_5	a_6	a_7	a_8
OC [20]	0.18897	0.595	0.16	0.577	0.09534	0.754	0.08504	0.732
OC fitting	0.2011	0.538	0.1141	0.7539	0.0794	0.6992	0.1285	0.5178

Figure 6 shows the results for Owens Corning fibre with $\rho_f = 157 \text{ kg/m}^3$. Experimental results are compared with theoretical predictions. The resistivity has been calculated with the Equation 3 where $A_1 = 1.083099$ and $A_2 = 1.82587$ [20]. These coefficients correspond to a resistivity of $4896 \text{ N}\cdot\text{s/m}^4$ and $17378 \text{ N}\cdot\text{s/m}^4$ for a $\rho_f = 100 \text{ kg/m}^3$ and $\rho_f = 200 \text{ kg/m}^3$ respectively, assuming a temperature of 25°C .

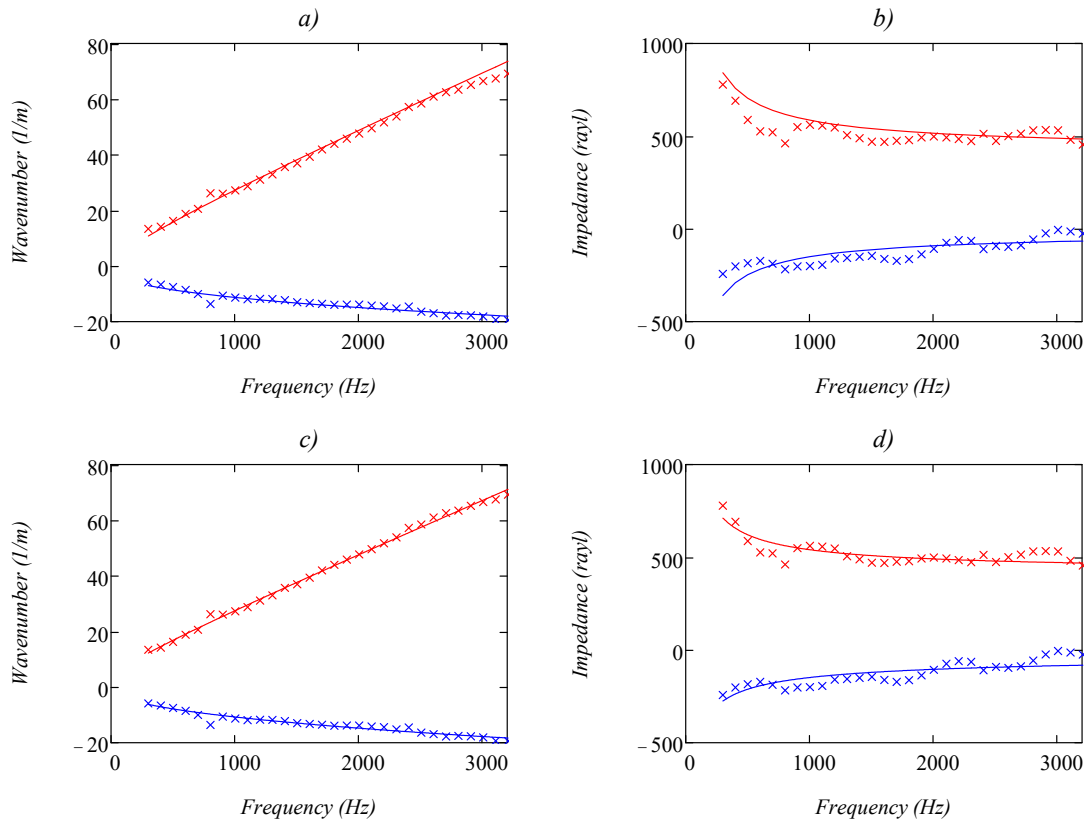


Figure 6 Fibreglass $\rho_f = 157 \text{ kg/m}^3$: a) wavenumber [20], b) impedance [20], c) wavenumber optimized, d) impedance optimized; —, theoretical real part; $\times \times$, experimental real part; —, theoretical imaginary part; $\times \times$, experimental real part.

As expected, there is a considerable similarity between the classical and the optimized model due to the fact of the acoustic behaviour of this material is well known.

The small differences between the coefficients are not very relevant since the behaviour are close enough. Therefore the procedure can be considered adequate.

5.1.2 Natural fibres

The results of the different optimization processes applied to the natural fibres are shown in Table 4, where the usual values used by Garai [16] are also presented.

Table 4 Comparison of Delany&Bazley's coefficients for natural fibres.

	a_1	a_2	a_3	a_4	a_5	a_6	a_7	a_8
Garai	0.159	0.571	0.121	0.53	0.078	0.623	0.074	0.66
Coconut fitting	0.1631	0.5849	0.1703	0.7274	0.2921	0.0431	0.1165	0.011
Coconut-sisal fit.	0.1314	0.5574	0.1119	0.7446	0.2607	0.01	0.1018	0.096

Figure 7 and 8 show the results for coconut and coconut-sisal fibre. Experimental results are compared with theoretical predictions.

If the results shown in Figures 7 c) and 7 d) obtained through an optimization curve fitting are compared to those achieve using Garai's coefficients (Figures 7 a) and 7 b)), it can be observed that the first considerably improves the estimation of the acoustical properties. The same conclusion can be inferred from Figure 8 that corresponds to coconut-sisal fibre.

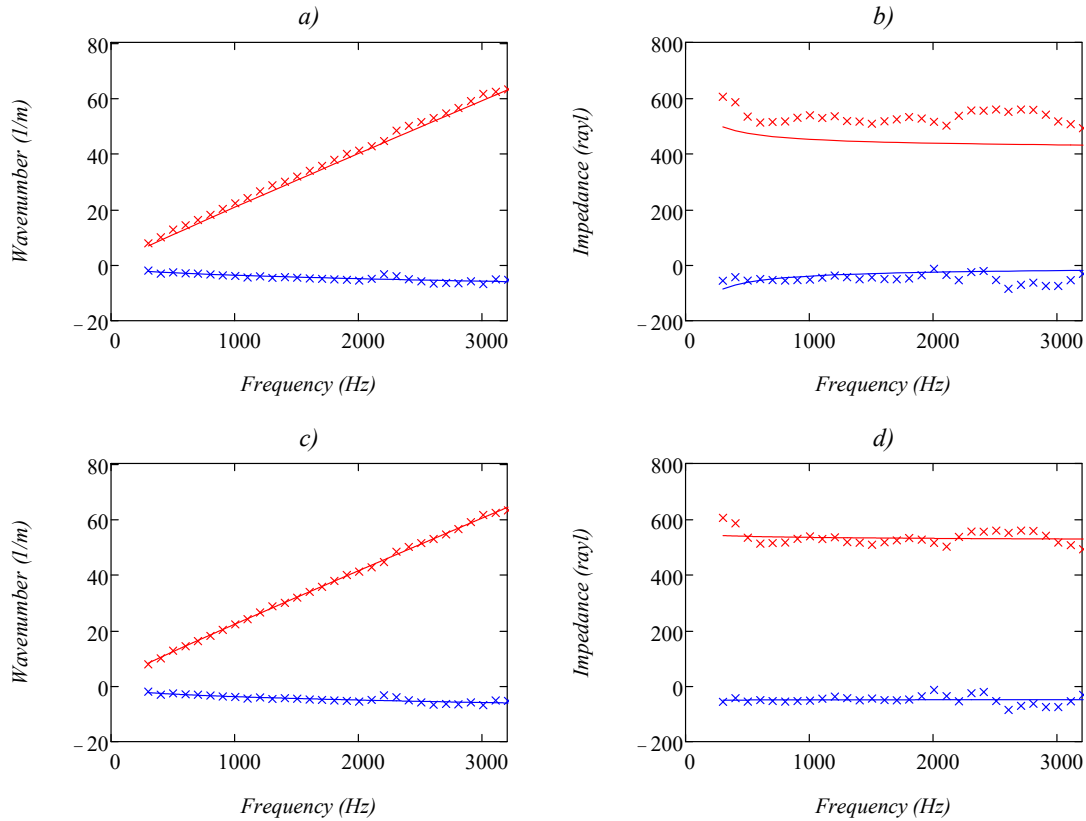


Figure 7 Coconut fibre $\rho_f = 87.3 \text{ kg/m}^3$: a) wavenumber [16], b) impedance [16] c) wavenumber with optimized coefficients, d) impedance with optimized coefficients; —, theoretical real part; $\times \times$, experimental real part; —, theoretical imaginary part; $\times \times$, experimental real part.

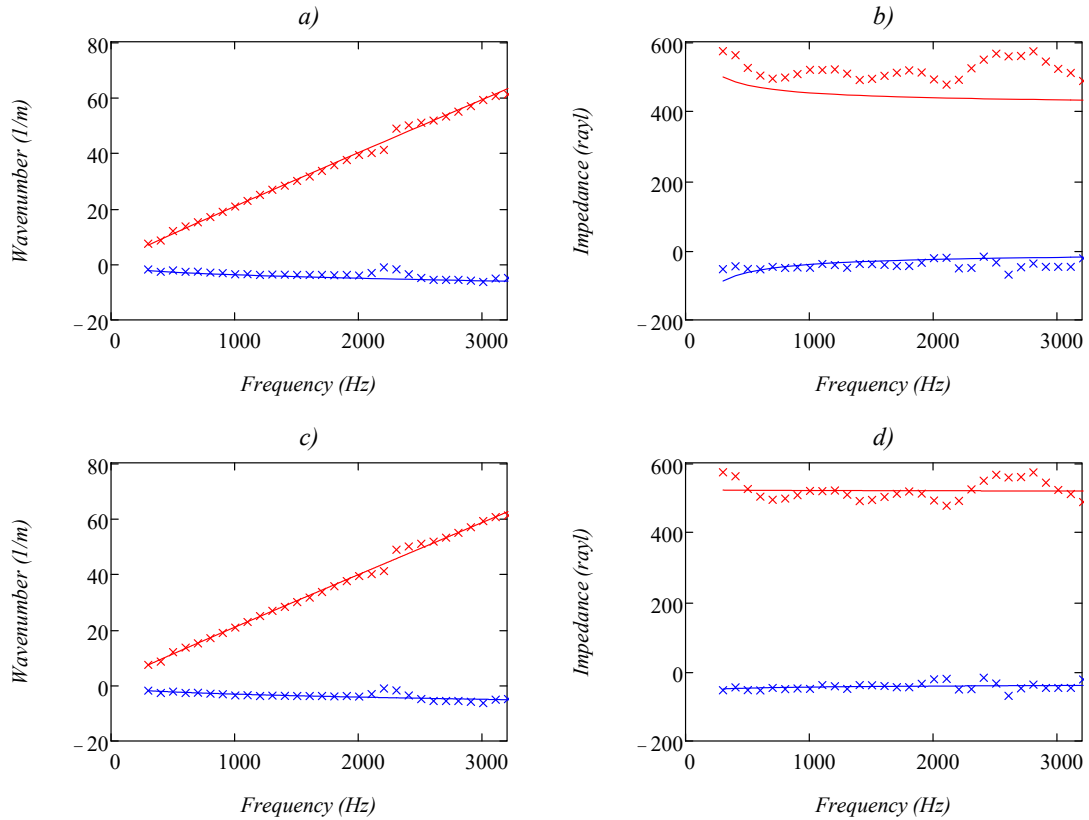


Figure 8 Coconut-sisal fibre $\rho_f = 95.7 \text{ kg/m}^3$: a) wavenumber [16], b) impedance [16] c) wavenumber with optimized coefficients, d) impedance with optimized coefficients; —, theoretical real part; $\times \times$, experimental real part; —, theoretical imaginary part; $\times \times$, experimental real part.

5.2 Practical application of natural fibres

With the purpose of checking the validity of the proposed methodology, a prototype of a dissipative silencer with coconut fibre has been constructed. Its TL [21] is measured and also calculated with the new coefficients (see Table 2 and 4). Figure 9 shows the prototype and its dimensions.

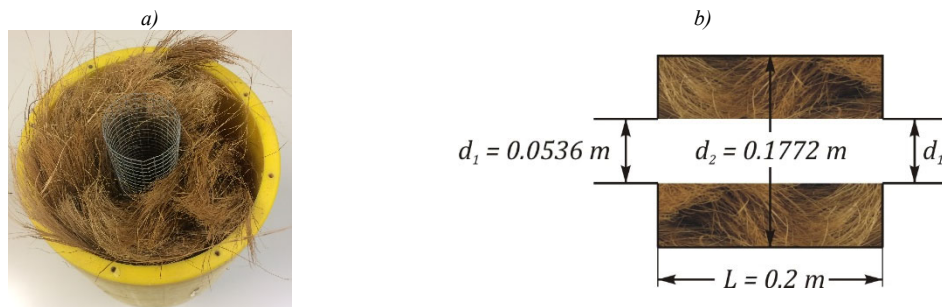


Figure 9 Dissipative silencer with coconut fibre: a) prototype; b) dimensions.

Figure 10 shows the TL obtained from experimental measurements using the two source method with simultaneous excitation [22]. The numerical prediction has been obtained by means of FEM calculations with an in-house code developed by the authors [8].

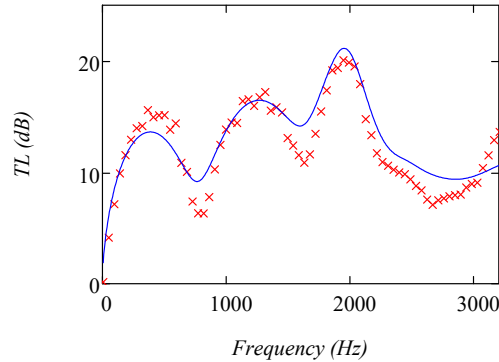


Figure 10 TL of a dissipative silencer with coconut fibre with $\rho_f = 60 \text{ kg/m}^3$; $\times \times$, experimental; —, numerical calculation with optimized coefficients.

Figure 10 shows that the numerical predictions and the experimental results present a similar trend. The discrepancies appearing between the TL curves can be due, among other reasons, to the uneven filling of the chamber with the coconut fibre since it is not easy to distribute it in a uniform way by hand as it can be deduced from Figure 9.

6. CONCLUSIONS

The static flow resistivity of coconut and coconut-sisal fibres has been measured following a procedure based on the corresponding standard. The values obtained for natural fibres are consistent with the results found in the bibliography. Later an experimental curve fitting method has been applied to adapt the Delany and Bazley model to the natural fibres. The wavenumber and the impedance calculated with the new coefficients show good agreement with measurements. The new models have been employed to calculate the TL of a dissipative silencer constructed with coconut fibre through FEM. Measurements and computations show a similar trend.

7. ACKNOWLEDGEMENTS

The authors gratefully acknowledge the financial support of Ministerio de Ciencia, Innovación y Universidades – Agencia Estatal de Investigación and the European Regional Development Fund (project TRA2017-84701-R), as well as Generalitat Valenciana (project Prometeo/2016/007).

8. REFERENCES

1. <https://www.who.int> (Retrieved February 2018)
2. M.H.F. De Salis, D.J. Oldham and S. Sharples, “Noise control strategies for naturally ventilated buildings”, *Building and Environment*, 37, 471-484 (2002).
3. R. Barron, “*Industrial noise control and acoustics*”, Marcel Dekker, New York (2003).
4. C. Bibby and M. Hodgson, “Field measurement of the acoustical and airflow performance of interior natural-ventilation openings and silencers”, *Building and Environment*, 67, 265-273 (2013).
5. Z.H. Wang, C.K. Hui and C.F. Ng, “The acoustic performance of ventilated window with quarter-wave resonators and membrane absorber”, *Applied Acoustics*, 78, 1-6 (2014).
6. F.D. Denia, E.M. Sánchez-Orgaz, J. Martínez-Casas and R. Kirby, “Finite element based acoustic analysis of dissipative silencers with high temperature and thermal-induced heterogeneity”, *Finite Elements in Analysis and Design*, 101, 46-57 (2015).

7. E.M. Sánchez Orgaz, F.D. Denia, J. Martínez-Casas and L. Baeza, “*Efficient approaches for the acoustic modelling of automotive exhaust devices. Application to configurations incorporating granular materials and monoliths*”, ICSV 24, London-United Kindom (2018).
8. E.M. Sánchez-Orgaz, “*Advanced numerical techniques for the acoustic modelling of materials and noise control devices in the exhaust system of internal combustion engines*”, Ph Thesis, Universitat Politècnica de València (2016).
9. S. Allam and M. Åbom, “*A new type of muffler based on microperforated tubes*”, Journal of Vibration and Acoustics, 133, 1-8 (2011).
10. A. Navacerrada, C. Díaz, A. Pedrero, M. Isaza, P. Fernández, C. Álvarez-López and A. Restrepo-Osorio, “*Caracterización acústica y térmica de no tejidos basados en fibras naturales*”, EuroRegio 2016, Porto-Portugal (2018).
11. J.P. Arenas and M.J. Crocker, “*Recent trends in porous sound-absorbing materials*”, Sound & Vibration, 44, 12-17 (2010).
12. A.M. Pedrosa, E.M. Sánchez Orgaz, F.D. Denia and F.J. Fuenmayor “*Caracterización acústica de fibras naturales fonoabsorbentes mediante una técnica experimental de dos fuentes con excitación simultánea*”, FIA 2018, Cádiz-Spain (2018).
13. A.M. Pedrosa, “*Desarrollo de herramientas experimentales para la caracterización acústica de silenciadores en presencia de flujo medio*”, Ph Thesis, Universitat Politècnica de València (2015).
14. M.E. Delany and E. N. Bazley, “*Acoustical properties of fibrous absorbent materials*”, Applied Acoustics, 3, 105-116 (1970).
15. F.D. Denia, A. Selamet, F.J. Fuenmayor and R. Kirby, “*Acoustic attenuation performance of perforated dissipative mufflers with empty inlet/outlet extensions*”, Journal of Sound and Vibration, 302, 1000-1017 (2007).
16. M. Garai and F. Pompili, “*A simple empirical model of polyester fibre materials for acoustical applications*”, Applied Acoustics, 66, 1383-1398 (2005).
17. U. Berardi and G. Iannace “*Acoustic characterization of natural fibers for sound absorption applications*”, Building and Environment, 94, 840-852 (2015).
18. ISO 9053-1, “*Acoustics - Determination of airflow resistance – Part 1: Static airflow method*” (2018).
19. R.J. Del Rey, J. Alba, J.P. Arenas and J. Ramis, “*Evaluation of two alternative procedures for measuring airflow resistance of sound absorbing materials*”, Archives Acoust. 38 (4) (2013) 547-554
20. A.G. Antebas, F.D. Denia, A.M. Pedrosa and F.J. Fuenmayor, “*A finite element approach for the acoustic modeling of perforated dissipative mufflers with non-homogeneous properties*”, Mathematical and Computer Modelling. 57 (2013) 1970–1978
21. Munjal, M.L. “*Acoustics of ducts and mufflers*”, Wiley-Interscience, Nueva York (2014).
22. A.M. Pedrosa, F.D. Denia, A.J. Besa and F.J. Fuenmayor, “*A two source method with simultaneous excitation for the acoustic characterization of exhaust systems with mean flow*”, Internoise 2013, Innsbruck-Austria (2013).